Biological oxygen productivity during the last 60,000 years from triple oxygen isotope measurements

Thomas Blunier,[1] Bruce Barnett, Michael L. Bender, and Melissa B. Hendricks
Department of Geosciences, Princeton University, Princeton, New Jersey, USA

Received 5 July 2001; revised 8 February 2002; accepted 8 February 2002; published 3 July 2002.

[1] The oxygen isotope signature of atmospheric O_2 is linked to the isotopic signature of seawater (H_2O) through photosynthesis and respiration. Fractionation during these processes is mass dependent, affecting $\delta^{17}O$ about half as much as $\delta^{18}O$. An "anomalous" fractionation process, which changes $\delta^{17}O$ and $\delta^{18}O$ of O_2 about equally, takes place during isotope exchange between O_2 and CO_2 in the stratosphere. The relative rates of biologic O_2 production and stratospheric processing determine the relationship between $\delta^{17}O$ and $\delta^{18}O$ of O_2 in the atmosphere. Variations of this relationship thus allow us to estimate changes in the rate of mass-dependent O_2 production by photosynthesis versus the rate of O_2-CO_2 exchange in the stratosphere with about equal fractionations of $\delta^{17}O$ and $\delta^{18}O$. In this study we reconstruct total oxygen productivity for the last glacial, the last glacial termination, and the early Holocene from the triple isotope composition of atmospheric oxygen trapped in ice cores. With a box model we estimate that total biogenic productivity was only $\sim$76–83% of today for the glacial and was probably lower than today during the glacial-interglacial transition and the early Holocene. Depending on how reduced the oxygen flux from the land biosphere was during the glacial, the oxygen flux from the glacial ocean biosphere was 88–140% of its present value. *INDEX TERMS:* 3344 Meteorology and Atmospheric Dynamics: Paleoclimatology; 4870 Oceanography: Biological and Chemical: Stable isotopes; 1615 Global Change: Biogeochemical processes (4805); 0315 Atmospheric Composition and Structure: Biosphere/atmosphere interactions; *KEYWORDS:* GISP2, SIPLE ice cores, oxygen isotopes, past oxygen productivity, stratospheric isotope exchange, respiration

1. Introduction

[2] Interactions between climate and the biosphere shape many fundamental properties of the environment. The most obvious example is the profound influence of climate on terrestrial vegetation. Less obviously, climate also influences ocean productivity through its effects on ocean circulation. Fertility thus tends to be high where vertical mixing brings nutrients to the surface.

[3] Properties of the biosphere also influence climate. The atmospheric CO_2 concentration, and thus the radiative forcing of CO_2, is lowered slightly as terrestrial biomass increases. Similarly, production of biomass in the oceans and its vertical export to depth lowers the partial pressure of CO_2 in the surface ocean and thus lowers the concentration of CO_2 in air [e.g., *Broecker*, 1982; *Sigman and Boyle*, 2000]. The land biosphere also has a direct influence on climate. For example, vegetation lowers albedo and increases the recycling of water by evapotranspiration [e.g., *Kleidon et al.*, 2000]. Provocative recent work links diminished vegetation to greater atmospheric erosion of dust and its higher fallout over the ocean. Increased dust fluxes may lead to greater ocean productivity and lower CO_2, cooler climates, and sparser vegetation [*Cowling and Sage*, 1998; *Fung et al.*, 2000; *Mahowald et al.*, 1999; *Martin*, 1990]. Data and modeling studies suggest that all these processes may be important at glacial-interglacial timescales [e.g., *de Noblet et al.*, 1996; *Gallimore and Kutzbach*, 1996; *Kutzbach et al.*, 1996; *Cowling and Sage*, 1998; *Fung et al.*, 2000; *Mahowald et al.*, 1999; *Martin*, 1990].

[4] The object of this paper is to quantify one critical property of the biosphere during the last ice age: the rate of photosynthetic O_2 production. This property is a measure of the fertility of the biosphere and gives insight into the nature of the biosphere during glacial times.

[5] At the outset, we need to acknowledge limits to the insight we can gain about the biosphere by knowing gross O_2 production during the last ice age. First, the productivity terms of greatest interest are land productivity and ocean productivity as independent values. Our parameter gives an estimate of the total productivity but gives limited information on the individual contributions. Second, even if we were able to separate productivities, the results would still have limitations. The most important rate term for land carbon production is net primary production. This is significantly less than gross photosynthetic O_2 production, although the terms can be related by invoking estimates of plant mitochondrial respiration, photorespiration, and the

[1] Now at Climate and Environmental Physics, Physics Institute, University of Bern, Bern, Switzerland.

0886-6236/02/2001GB001460$12.00

Mehler reaction. An important term for ocean fertility is new production (which is similar to net or export production). This rate is far less than gross O_2 production, and there is no simple link between the two terms.

[6] In this paper we constrain gross primary production during the Holocene and the last ice age by measuring the relative abundance of the three stable oxygen isotopes, ^{16}O, ^{17}O, and ^{18}O, in O_2 of fossil air trapped in ice cores [*Luz et al.*, 1999]. The isotopic composition of O_2 in air depends almost entirely on isotopic fractionation during respiration and on the hydrologic processes that influence the isotopic composition of leaf water [e.g., *Bender et al.*, 1994]. *Luz et al.* [1999], however, showed that the isotopic composition of the atmosphere also has a small but distinctive perturbation derived from photochemical reactions in the stratosphere. It manifests itself as a small decrease in the $\delta^{17}O$ and $\delta^{18}O$ of O_2 in air. More importantly, the perturbation causes a deviation in the relationship between $\delta^{17}O$ and $\delta^{18}O$ of O_2 (normally, $\delta^{17}O$ is fractionated about half as much as $\delta^{18}O$). The magnitude of the tropospheric perturbation reflects relative rates of photosynthesis and stratospheric photochemistry. We quantify changes in the latter rate, allowing us to estimate changes in past rates of photosynthesis.

[7] Changes in the global fractionation of O_2 by the processes of respiration and hydrology can also induce subtle changes in the relationship between $\delta^{17}O$ and $\delta^{18}O$ of O_2. Understanding these metabolic and hydrologic changes is essential, because they can mask part of the stratospheric perturbation or can appear to enhance it. These changes come about because normal, mass-dependent processes actually fractionate ^{17}O by slightly more than 0.5 times as much as ^{18}O. The exact ratio varies by about ±0.01 for different processes. We develop a formalism that accounts for the influence of respiration and hydrology on the triple isotope composition of O_2. We then use this formalism to derive past rates of gross O_2 production. We also discuss constraints of our work for the ice age partitioning of gross O_2 production between the ocean and the land biosphere.

2. Triple Isotope Systematics of O_2

[8] Nominal abundances of oxygen isotopes ^{16}O, ^{17}O, and ^{18}O are 99.76, 0.04, and 0.20%, respectively. Variations in the isotopic composition are measured as deviations from a standard in per mil (equation (1)) where ${}^{x}R_{SA}$ and ${}^{x}R_{ST}$ are ratios of $[^{18}O^{16}O]/[^{16}O_2]$ (x = 18) and $[^{17}O^{16}O]/[^{16}O_2]$ (x =17) for sample and standard, respectively.

$$\delta(‰) = \left(\frac{{}^{x}R_{SA}}{{}^{x}R_{ST}} - 1\right)1000. \quad (1)$$

[9] Fractionation factors α are defined by equation (2), where R_A and R_B are ratios in reactant and product associated with an instantaneous isotope exchange reaction.

$$R_B = \alpha R_A. \quad (2)$$

[10] By analogy we also use α to describe the overall fractionation of several isotope exchange reactions. The isotope effect from an isotope exchange reaction with fractionation factor α is

$$\varepsilon(‰) = (\alpha - 1)1000. \quad (3)$$

Here ε equals the delta value of B if A is the standard.

[11] Two sets of reactions alter the isotopic composition of atmospheric O_2. The first involves the biological processes of photosynthesis and respiration. The second is the photochemically induced exchange of O atoms between O_2 and CO_2, which occurs mainly in the stratosphere. Biological reactions dominate the turnover of O_2 and are the primary influence on its isotopic composition. Stratospheric processes, however, introduce the signal critical to this study.

[12] Today the $\delta^{18}O$ of atmospheric O_2 is 23.50‰ heavier than ocean water, here taken as standard mean ocean water (SMOW) [*Kroopnick and Craig*, 1972]. This difference represents the steady state composition at which the $\delta^{18}O$ of O_2 produced by photosynthesis and the stratospheric exchange reaction equals the $\delta^{18}O$ of O_2 consumed by respiration. The O_2-seawater difference is called the Dole effect [*Lane and Dole*, 1956]. During the past 400,000 years the Dole effect has been relatively constant, with little change observed between glacial and interglacial periods [*Bender et al.*, 1994; *Shackleton*, 2000].

[13] Photosynthesis converts oxygen of H_2O to O_2 with essentially no isotopic fractionation [*Guy et al.*, 1993]. In contrast, respiration discriminates against the heavy isotope by ~18–20‰ [*Guy et al.*, 1992, 1993; *Kiddon et al.*, 1993], leaving O_2 enriched in the heavy isotope. Steady state between these two processes is achieved when $\delta^{18}O$ of O_2 produced by photosynthesis equals $\delta^{18}O$ of O_2 consumed by respiration. This is the case when atmospheric oxygen reaches a $\delta^{18}O$ of ~18–20‰, clearly less than the observed Dole effect of 23.50‰. A first-order correction comes from the fact that ~65% of the photosynthetic O_2 production takes place in leaves of land plants. Leaf water derives from precipitation. Precipitation is depleted in $\delta^{18}O$ relative to SMOW [e.g., *Craig and Gordon*, 1965]. Evapotranspiration, however, leads to a $\delta^{18}O$ enrichment in leaf water because $H_2{}^{16}O$ evaporates more rapidly. The ^{18}O enrichment due to evapotranspiration exceeds the ^{18}O depletion of precipitation. Consequently, leaf water, and therefore photosynthetic O_2 produced from this water, is enriched in ^{18}O relative to SMOW by 4–8‰ [*Farquhar et al.*, 1993; *Yakir et al.*, 1994]. This effect raises the $\delta^{18}O$ of O_2 close to the observed value.

[14] A number of second-order effects have a small but significant influence on the magnitude of the Dole effect. These include the solubility fractionation of O_2 isotopomers [*Benson and Krause*, 1984], different isotope effects associated with different pathways of metabolic O_2 consumption [*Guy et al.*, 1993], and partial recycling of O_2 in subsurface ocean waters [*Bender et al.*, 1994].

[15] The processes of biology, hydrology, and dissolution fractionate isotopes in a mass-dependent manner. For small fractionations the fractionation ratios of isotope pairs are approximately equal to the ratios of the difference of the reciprocal masses of the substituted atom [*Hulston and Thode*, 1965]. For oxygen this means that $\delta^{17}O$ is fractionated about half as much as $\delta^{18}O$.

[16] *Mook* [2000] describes the general relation between isotope pairs as

$$\left(\frac{^{m_1}R_A}{^{m_1}R_B}\right) = \left(\frac{^{m_2}R_A}{^{m_2}R_B}\right)^{\lambda}$$
$$^{m_1}\alpha = (^{m_2}\alpha)^{\lambda}, \quad (4)$$

where ^{m_1}R and ^{m_2}R are isotope ratios for $^{m_1}X/^{m_0}X$ and $^{m_2}X/^{m_0}X$. Subscripts A and B stand for instantaneous ratios of reactants and products, respectively. The fractionation ratio λ varies slightly for different reactions. Therefore the ratio of $\delta^{17}O$ to $\delta^{18}O$ in accumulated products will vary with the reactions involved. However, the nature of the relationship depends equally on the nature of the fractionation process.

[17] As an example, we derive the relation for Rayleigh distillation. Consider the progressive condensation of water liquid from vapor in a closed system. Equation (5) applies, where $^xR = [^xO^{16}O]/[^{16}O_2]$ and x stands for 18 or 17; R_V is the isotope ratio of the remaining water vapor, R_{V0} is the initial isotope ratio of the vapor, and $^x\alpha$ is the fractionation associated with condensation.

$$\frac{^xR_V}{^xR_{V0}} = f^{^x\alpha - 1}, \quad (5)$$

where f is the fraction of initial water vapor remaining as gas [e.g., *Hoefs*, 1997]. One can then solve equations for both ^{17}O and ^{18}O for f, set the solutions equal, and derive equation (6) for the case of Rayleigh distillation.

$$\left(\frac{\delta^{17}O}{10^3} + 1\right) = \left(\frac{\delta^{18}O}{10^3} + 1\right)^{\gamma}, \quad (6)$$

where $\gamma = (^{17}\alpha - 1)/(^{18}\alpha - 1)$. Note that the exponent γ is not equal to λ as defined in equation (4).

[18] The fractionation of O isotopes in the meteoric water cycle, which influences the isotopic composition of source waters for land photosynthesis, is largely a Rayleigh process. *Li and Meijer* [1998] showed that the $\delta^{17}O$-$\delta^{18}O$ ratio of precipitation water follows a function of the form given in equation (6) with $\gamma = 0.5281$.

[19] *Luz et al.* [1999] measured the covariance of $\delta^{18}O$ and $\delta^{17}O$ due to respiration in a terrarium experiment. They found that the $\delta^{17}O$ versus $\delta^{18}O$ trend has a slope of 0.521 where atmospheric oxygen is the standard. This slope is standard dependent. However, the dependence of $\delta^{17}O$ and $\delta^{18}O$ can be formulated in a standard-independent way using equation (6) with a $\gamma = 0.518$ (B. Luz, personal communication, 2001). Equation (6) with $\gamma = 0.518$ is equivalent to a linear relation with slope 0.521 and atmospheric oxygen being the standard. The main process fractionating atmospheric oxygen is respiration. Consequently, following the approach of *Luz et al.* [1999], we use the $\delta^{17}O$ versus $\delta^{18}O$ trend of respiration to define $\Delta^{17}O$, the deviations from normal, mass-dependent fractionation. $\Delta^{17}O$ is expressed in terms of per meg (1 per meg = 0.001‰) as

$$\Delta^{17}O(\text{per meg}) = \left[\delta^{17}O(‰) - 0.521\delta^{18}O(‰)\right]1000. \quad (7)$$

[20] It is important to recognize that equation (7) is a definition. $\Delta^{17}O$ will be nearly zero for properties fractionated by mass-dependent processes only. Even for normal mass-dependent processes, there will be small deviations from zero. First, there will be offsets associated with variations of λ for different reactions. Second, geochemical processes, such as Rayleigh distillation, can cause $\Delta^{17}O$ to deviate from zero even when ^{17}O and ^{18}O are fractionated with the λ for respiration.

[21] In the case of atmospheric O_2, the small deviations in $\Delta^{17}O$ introduced by biology and hydrology are superimposed on larger variations due to isotope exchange between O_2 and CO_2 in the stratosphere [*Bender et al.*, 1994; *Luz et al.*, 1999]. Oxygen isotopes are fractionated about equally during the formation of ozone (equations (8) and (9)), rather than by the common 1:2 ratio. The origin of this "mass-independent" isotope effect is still debated [see *Gao and Marcus*, 2001; *Mauersberger et al.*, 1999; *Thiemens*, 1999; *Weston*, 1999, and references therein]. In any case, the anomalously fractionated oxygen in O_3 is transferred to CO_2 by reactions shown in equations (10), (11), (12), and (13) [*Yung et al.*, 1991]. There may be an additional fractionation during the exchange reaction between $O(^1D)$ and CO_2 [*Barth and Zahn*, 1997].

$$O_2 + h\nu \rightarrow 2O, \quad (8)$$
$$O + O_2 \rightarrow O_3, \quad (9)$$
$$O_3 + h\nu \rightarrow O_2 + O(^1D), \quad (10)$$
$$CO_2 + O(^1D) \rightarrow CO_3, \quad (11)$$
$$CO_3 \rightarrow CO_2 + O, \quad (12)$$
$$O + O \rightarrow O_2. \quad (13)$$

[22] In equation (10), anomalously fractionated ozone is photolyzed into molecular oxygen and an excited oxygen atom that is also anomalously enriched in the heavy isotopes. In equation (11) this oxygen atom reacts with CO_2. The three O atoms in CO_3 are thought to be equivalent [*Yung et al.*, 1991], and CO_3 randomly loses one oxygen atom (equation (12)). Therefore CO_3 has a 67% chance to retain its O atom derived from O_2 and release an O atom that was present in the predecessor CO_2 molecule. The reaction sequence (equations (8), (9), (10), (11), (12), and (13)) thus leads to exchange of O atoms between O_2 and CO_2 in the absence of net chemical fluxes. Exchange of O leads to isotope fractionation between O_2 and CO_2. Heavier isotopes are transferred to CO_2. What is significant for our purposes is that this fractionation does not follow the "normal" $^{17}\varepsilon/^{18}\varepsilon$ ratio of ~0.5. As for ozone, the fractionation is anomalous in the sense that the $\delta^{17}O$ of CO_2 increases by much more than $\sim 0.5\delta^{18}O$. In turn, the $\delta^{17}O$ of O_2 decreases by more than ~0.5 times the $\delta^{18}O$ decrease. The formation rate of anomalous O_2 is determined by the amount of O_3 and CO_2 in the stratosphere and by the rate of O_3 photolysis.

[23] We infer that $\delta^{17}O$ of O_2 becomes anomalously low at the same rate as $\delta^{17}O$ of CO_2 becomes anomalously high, scaled by the concentration ratio of CO_2 to O_2 (currently 370/210,000 ppmv) [*Gamo et al.*, 1989; *Thiemens et al.*, 1991]. The stratosphere to troposphere gradient of $\Delta^{17}O$ of O_2 is very small. The isotopic composition of O_2 has never

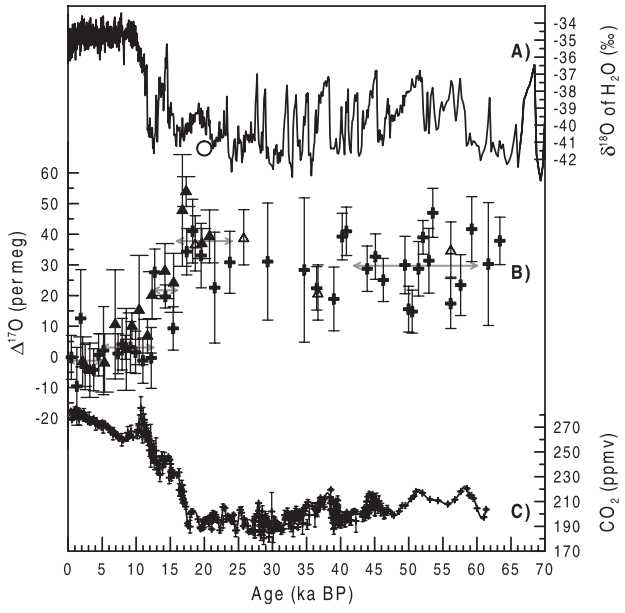

Figure 1. Results from the Greenland Ice Sheet Project 2 (GISP2) and Siple Dome ice cores. (a) $\delta^{18}O$ of the ice, a proxy for local temperature [*Grootes et al.*, 1993] from the GISP2 ice core, Greenland. (b) $\Delta^{17}O$ values, where open triangles are results from *Luz et al.* [1999] and crosses and solid triangles are individual measurements from GISP2 and Siple Dome, respectively. Shaded arrows indicate periods and mean values for late Holocene (0–5 ka), early Holocene (5–12.5 ka), the transition from the last glacial to the Holocene (12.5–16 ka), the last glacial maximum (16–24 ka) and the midglacial (42–60 ka). (c) Composite record of atmospheric CO_2 from the Taylor Dome and the Byrd station ice cores, Antarctica [*Indermühle et al.*, 2000; *Indermühle*, 1999; *Stauffer et al.*, 1998]. $\Delta^{17}O$ data from GISP2 and Siple Dome are available from the National Oceanic and Atmospheric Administration Geophysical Data Center (www.ngdc.noaa.gov/paleo/paleo.html). Open circle shows an illustrative result of our model calculation (see text for model details). Using the modern biological O_2 productivity together with a Last Glacial Maximum (LGM) CO_2 level and LGM isotope ratios for seawater results in a $\Delta^{17}O$ of approximately +70 per meg as opposed to the observed +38 per meg.

been measured to the high precision required to identify this gradient.

[24] Anomalous oxygen formed in the stratosphere accumulates in the atmosphere. An oxygen molecule cycles through the stratosphere nominally ~24 times before it is consumed by respiration. This number is equal to the ratio of the turnover time of O_2 in air with respect to biology (~1200 years) to the time required for the global atmosphere to cycle through the stratosphere (~50 years). The result is that ocean water has a $\delta^{17}O$ of 249 per meg versus atmosphere [*Luz and Barkan*, 2000]. This translates to atmospheric O_2 having a $\Delta^{17}O$ of −391 per meg versus ocean water, applying the current atmospheric $\delta^{18}O$ value of 23.50‰ versus SMOW [*Kroopnick and Craig*, 1972] and the isotope ratios for SMOW reported by *Hoefs* [1997].

[25] The relative value of $\delta^{17}O$ and $\delta^{18}O$ in the atmosphere is determined by the relative influence of mass-dependent, mainly biological, processes versus anomalous processes in the stratosphere. Therefore coupled values of $\delta^{17}O$ and $\delta^{18}O$ give us a measure of biological oxygen production, relative to O_2 cycling rates in the stratosphere [*Luz et al.*, 1999]. We adopt O_2 in ambient air as the isotopic standard for $\delta^{17}O$ and $\delta^{18}O$. Therefore $\Delta^{17}O$ presently has a value of 0 per meg by definition.

3. Measurements

[26] We measured $\Delta^{17}O$ in trapped air samples from the Greenland Ice Sheet Project 2 (GISP2) (38.48°W, 72.58°N) ice core drilled between 1989 and 1993 and the Siple Dome ice core drilled in 1996–1999 (81.66°S, 181.81°W). For each measurement, ~70 g of ice was used to yield roughly 7 mL of air standard temperature and pressure. Air extractions were made by a melt-refreezing method with a recovery efficiency of ~99%. Samples were processed following the approach from *Luz et al.* [1999], in which extracted air is chromatographed to quantitatively separate O_2 and Ar from N_2. The air sample is transferred from the extraction chamber, chilled to −60°C, and condensed on coarse (2 mm diameter) type 5Å mol sieve held at liquid nitrogen temperature. The full sample is then injected on a chromatography column (mol sieve 5Å, 4 m, 1/8″, 60/80 mesh) at 40°C. The eluting O_2/Ar mixture is then trapped on a second mol sieve trap held at liquid nitrogen temperature (5Å, 45/60 mesh). All other components of the sample are directed to waste. Carrier gas of grade 5.0 helium was cleaned of contaminants with a mol sieve trap cooled by liquid nitrogen. A flow of 30 mL min^{-1} was used for the gas chromatographic separation. From the second trap, the sample is separated from the carrier gas by pumping the helium away while keeping the trap cold. The O_2/Ar mixture is then transferred to a stainless steel tube cooled to 20°K by a He refrigerator.

[27] Samples were analyzed on a Finnigan Mat 252 dual inlet mass spectrometer system. The $\Delta^{17}O$ from the mean of replicates was ±10 per meg, comparable to the results from *Luz et al.* [1999]. All data presented here have been corrected for gravitational enrichment in the firn quantified by $\delta^{15}N$ of N_2 measurements [*Schwander et al.*, 1997, also unpublished data]. The gravitational correction for $\delta^{17}O$ is 0.500 times that for $\delta^{18}O$ [*Schwander*, 1989]. The correction is on the order of 0.3‰ for $\delta^{17}O$, 0.6‰ for $\delta^{18}O$, and 10–15 per meg for $\Delta^{17}O$. Our working standard is air collected in 1994 from a site far from pollution sources and representative of the troposphere with respect to O_2.

4. Results

[28] Figure 1 shows the $\Delta^{17}O$ results for the GISP2 and Siple Dome ice cores back to 70 ka. Results from the two ice cores agree within the uncertainty of the measurements. Our results also agree well with four samples analyzed in duplicate by *Luz et al.* [1999] from GISP2 in the time range of our measurements.

[29] We averaged our results over several time intervals. For the midglacial (60–42 ka) we obtain mean $\Delta^{17}O$ values

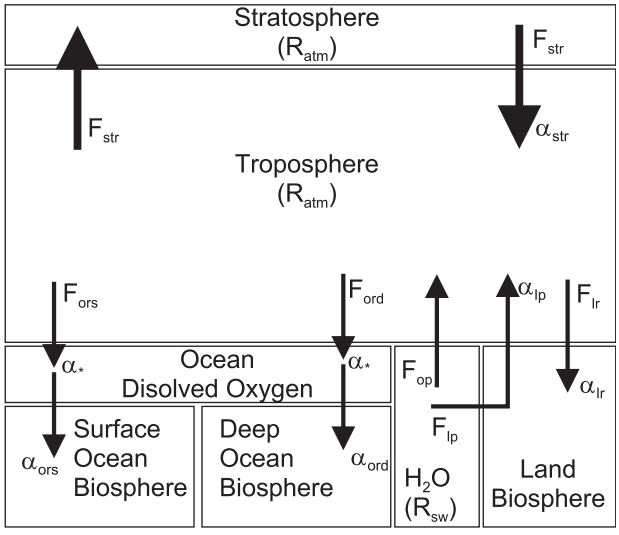

Figure 2. Sketch of our box model. Arrows indicate fluxes (F) of oxygen where a at the tips of the arrows are the fractionation factor associated with oxygen flux. R are isotope ratios of $[^{18}O^{16}O]/[^{16}O_2]$ or $[^{17}O^{16}O]/[^{16}O_2]$.

of atmospheric O_2 of +30 per meg. For the last glacial maximum (LGM) (here taken as 24–16 ka), $\Delta^{17}O$ values average +38 per meg. Then $\Delta^{17}O$ values decrease to ~3 per meg in the early Holocene, and to −1 per meg in the late Holocene (5–0 ka). The deglacial $\Delta^{17}O$ decrease parallels the deglacial CO_2 increase and the deglacial warming observed in Antarctica.

[30] Here we present a brief, qualitative interpretation of our data, which foreshadows the quantitative assessment of section 5. The higher $\Delta^{17}O$ values of glacial times are the result of two counterbalancing effects. First, atmospheric CO_2 was lower during glacial times. With less CO_2 available for exchange, anomalously formed O_2 would have been produced less rapidly, and $\Delta^{17}O$ would rise toward its biological value. Second, biological productivity was lower during the last ice age. The biological influence would thus diminish, and $\Delta^{17}O$ would decrease. The data show that lower glacial CO_2 "won" over lower biological productivity, causing $\Delta^{17}O$ to be higher in the glacial. However, as we shall see, $\Delta^{17}O$ did not rise as much as it would have if production remained constant. $\Delta^{17}O$ of glacial O_2 thus preserves a robust signal of lower productivity during the last glacial. The effect of lower CO_2, together with the increased isotope ratios for seawater and unchanged biological productivity during the glacial, would have resulted in a glacial $\Delta^{17}O$ of approximately +70 per meg as opposed to the observed +38 per meg. This illustrative result has been calculated with the box model that will be introduced in section 5. This box model for $\delta^{18}O$ and $\delta^{17}O$ will be used for a detailed interpretation of $\delta^{17}O$ in terms of biological productivity in the past relative to present.

5. Box Model

5.1. Model Description

[31] The tropospheric mass balance for O_2 is described by differential equation (14), where F are fluxes of $[^{16}O_2]$, M is the total amount of oxygen in the troposphere, and t is time. In this model, O_2 is exchanged between the troposphere and three other pools: the ocean biosphere, the land biosphere, and the stratosphere.

$$d(M)/dt = F_{op} - F_{ors} - F_{ord} + F_{lp} - F_{lr} - F_{str} + F_{str}, \quad (14)$$

where F_{op} is the gross photosynthetic oxygen flux from the ocean biosphere, F_{ors} is oxygen consumption by ocean respiration in the upper layer of water in equilibrium with the atmosphere, F_{ord} is consumption in the ocean interior, F_{lp} is the gross photosynthetic flux from the land biosphere, F_{lr} is land respiration, and F_{str} is the oxygen exchange flux between the troposphere and the stratosphere. Oxygen is neither consumed nor produced in the stratosphere, and the flux into the stratosphere equals the flux out of the stratosphere. Figure 2 shows a sketch of the box model.

[32] The mass balance for oxygen isotopomers $[^{18}O^{16}O]$ and $[^{17}O^{16}O]$ can be described by differential equation (15) written in ratio notation. This implies the approximations that fluxes for $([^{16}O_2] + [^{17}O^{16}O])$ and $([^{16}O_2] + [^{18}O^{16}O])$ are equal to the $[^{16}O_2]$ flux. R are isotope ratios and α are fractionation factors. Superscript x has values of 18 or 17. Thus ${}^{18}R = [^{18}O^{16}O]/[^{16}O_2]$ and ${}^{17}R = [^{17}O^{16}O]/[^{16}O_2]$. Subscripts sw and atm denote isotope ratios of seawater and atmosphere, respectively. As with equation (14), equation (15) has three parts. The first part accounts for marine photosynthesis and respiration, the second part accounts for terrestrial photosynthesis and respiration, and the third part accounts for the stratospheric effect.

$$\begin{aligned} d(M\,{}^{x}R_{atm})/dt \cong\ & F_{op}\,{}^{x}R_{sw} - F_{ors}\,{}^{x}R_{atm}\,{}^{x}\alpha_{*}\,{}^{x}\alpha_{ors} \\ & - F_{ord}\,{}^{x}R_{atm}\,{}^{x}\alpha_{*}\,{}^{x}\alpha_{ord} + F_{lp}\,{}^{x}R_{sw}\,{}^{x}\alpha_{lp} \\ & - F_{lr}\,{}^{x}R_{atm}\,{}^{x}\alpha_{lr} - F_{str}\,{}^{x}R_{atm} \\ & + F_{str}\,{}^{x}R_{atm}\,{}^{x}\alpha_{s} \end{aligned} \quad (15)$$

5.1.1. Ocean

[33] Photosynthesis of the ocean biosphere produces an O_2 flux F_{op} with the isotopic composition of the source water [*Guy et al.*, 1993]. The isotopic composition of ocean photosynthetic O_2 is thus ${}^{x}R_{sw}$.

[34] Ocean respiration mainly consumes oxygen dissolved in the mixed layer. Since oxygen dissolved in the mixed layer exchanges rapidly with oxygen in the atmosphere, the mixed layer is close to isotopic equilibrium with the atmosphere. Thus oxygen in the upper, mixed ocean is fractionated from the atmospheric ratio by approximately the equilibrium fractionation factor α_*. The total consumption rate of oxygen in the ocean is the sum of a flux F_{ors} in the well-ventilated surface ocean and a flux F_{ord} in the deep ocean. Associated fractionation factors for surface and deep ocean are α_{ors} and α_{ord}, respectively. The α_{ors} is the biological fractionation factor associated with respiration. The α_{ord} is an effective fractionation factor that enfolds effects of ocean mixing as well as respiration [*Bender et al.*, 1994; *Bender*, 1990]. The α_{ord} expresses the effect of respiration in the ocean interior as it would be seen by an observer monitoring its impact on the concentration and isotopic composition of O_2 in the atmosphere [*Kroopnick and Craig*, 1976; *Kroopnick*, 1987].

[35] Respiratory fractionation factors for ^{18}O are relatively well known, and we adopt values from the literature [*Kiddon et al.*, 1993; *Bender et al.*, 1994]. Fractionation factors for ^{17}O have not been measured directly so far. We calculate respiratory fractionation factors for ^{17}O from fractionation factors for ^{18}O applying *Mook*'s [2000] relation between isotope pairs (equation (4)). We derive λ from the measured steady state $\Delta^{17}O$ value of 249 per meg of the terrarium experiment by *Luz and Barkan* [2000] and *Luz et al.* [1999]. In this closed system experiment, steady state is reached when photosynthesis produces O_2 at the same rate as it is consumed by respiration. Equation (16) describes the rate of change of O_2 with time.

$$\frac{dM}{dt} = F_P - F_R, \tag{16}$$

where F_P is the rate of photosynthesis, F_R is the rate of respiration, and M is the mass of oxygen in the terrarium. We can write the same equation for [$^xO^{16}O$],

$$\frac{dM\,{}^xR}{dt} = F_p\,{}^xR_{sw} - F_R\,{}^xR\,{}^x\alpha_R, \tag{17}$$

where $^xR_{sw}$ is the isotopic ratio of the water used for photosynthesis and ^xR is the isotopic ratio of oxygen consumed by respiration. For photosynthesis the isotopic composition of O_2 is identical to that of the source water [*Guy et al.*, 1993]. For respiration, oxygen is fractionated by the respiratory fractionation factor $^x\alpha_R$. At steady state, $F_P = F_R$, and equation (17) becomes $^xR_{sw} = {}^xR\,{}^x\alpha_R$. Applying the definition of $\Delta^{17}O$ (equation (7)) together with values for R_{sw} (ocean water) and R_{atm} (atmosphere) as described in section 5.2, we calculate λ (= 0.518) from $^{18}\alpha_R$ Here $^{18}\varepsilon_R$ is taken as 20‰ [*Kiddon et al.*, 1993]. Following *Mook*'s [2000] relation between isotope pairs (equation (4)) we now calculate respiratory fractionation factors for $^{17}\alpha_{ors}$ and $^{17}\alpha_{ord}$ from isotope effects of $\delta^{18}O$. Values of $^{18}\alpha_{ors}$ and $^{18}\alpha_{ord}$ are taken as 20‰ [*Kiddon et al.*, 1993] and 12‰ [*Bender et al.*, 1994], respectively.

[36] Respiration as used here refers to all modes of biological O_2 consumption: mitochondrial respiration, photorespiration, Mehler reaction, chlororespiration, and the alternative pathway. These pathways have different fractionation factors for ^{18}O, and they might also have different λ values. The respiratory λ value derived from *Luz and Barkan* [2000] and *Luz et al.* [1999] is an average value for an unquantified contribution from different pathways. We provisionally assume that the ratio is the same for all pathways of O_2 consumption.

[37] The isotope enrichment for oxygen dissolved in seawater relative to atmospheric O_2, $^{18}\varepsilon_*$, is 0.7‰ [*Benson and Krause*, 1984]. According to *Luz and Barkan* [2000], dissolved oxygen in equilibrium with the atmosphere has a $\Delta^{17}O$ value of +16 per meg, which gives a value for $^{17}\varepsilon_*$ of +0.3807‰. Thus, in the mixed layer, dissolved O_2 has $\delta^{18}O$ = 0.7‰ and $\delta^{17}O$ = 0.3807‰.

[38] The marine oxygen flux is calculated from global ^{14}C-based primary production of 4.04×10^{15} mol C yr^{-1} [*Field et al.*, 1998]. We scale ^{14}C production to marine gross oxygen production, taking 0.37 as the ratio of ^{14}C production to marine gross oxygen production. This is the average productivity ratio determined from paired ^{14}C and ^{18}O trace incubation experiments in the North Atlantic, equatorial Pacific, Indian Ocean, and Southern Ocean, measured in process studies of the U.S. Joint Global Ocean Flux Study program [*Bender et al.*, 1999, 2000; *Dickson et al.*, 2001; *Kiddon et al.*, 1995; M.-L. Dickson, personal communication, 2000]. We thus calculate a gross oxygen production, F_{op}, of 1.09×10^{16} mol O_2 yr^{-1}. The total oceanic respiratory flux is partitioned to a respiratory flux in the well-ventilated upper ocean (95%) and into the deep ocean (5%), according to *Bender et al.* [1994].

5.1.2. Land

[39] Photosynthesis by the land biosphere produces an oxygen flux F_{lp}. The isotopic composition is identical to that of the source water [*Guy et al.*, 1993], which is now leaf water. The source water for photosynthesis of the land biosphere has undergone fractionation during evaporation from the ocean, precipitation, and evapotranspiration in leaves. In equation (15) the sum of these fractionation processes is described with a factor $^x\alpha_{lp}$ versus ocean water. The oxygen produced thus has the signature $^xR_{sw}\,{}^x\alpha_{lp}$. Land respiration consumes an oxygen flux of F_{lr}. Respiration consumes oxygen with the atmospheric ratio R_{atm}, which is fractionated by α_{lr}.

[40] Equation (18) [*White*, 1989] gives the isotopic ratio of leaf water (R_E) and hence gives the ratio $^xR_{sw}\,{}^x\alpha_{lp}$ of photosynthetic O_2. It is assumed that leaf water is in steady state so that water evaporating from the leaf has the isotopic composition of water taken up through the stem. Equation (18) is based on the *Craig and Gordon* [1965] equation, which expresses the isotopic composition of water evaporating from a surface in terms of relative humidity and relevant isotope effects.

$$^xR_{sw}\,{}^x\alpha_{lp} = {}^xR_E = [{}^xR_S(1-h)^x\alpha_k + h^xR_V]^x\alpha_{eq}. \tag{18}$$

[41] The isotopic ratio of leaf water R_E depends on the isotopic signature of the stem water R_S, which can be taken as equal to the ratio of precipitation water. R_E also depends on the composition of atmospheric water vapor R_V. According to equation (18), equilibrium and kinetic isotopic fractionation between liquid and gaseous water, $^x\alpha_{eq}$ and $^x\alpha_k$, both contribute to the fractionation process. The contribution of equilibrium fractionation rises and kinetic fractionation falls, as relative humidity (h) varies from 0 to 1.

[42] We now proceed to adopt the isotopic values required to solve equation (18). *Farquhar et al.* [1993] calculate the $\delta^{18}O$ of average precipitation water to be −7.9‰. They also calculate that $\delta^{18}O$ of average atmospheric water vapor is 10.3‰ lower than precipitation water. They calculate average values by weighting regional $\delta^{18}O$ of precipitation and atmospheric water vapor by regional gross primary production. *Li and Meijer* [1998] show that $\delta^{18}O$ and $\delta^{17}O$ of precipitation water are related by equation (6) with γ = 0.5281. We calculate $^{17}R_S$ and $^{17}R_V$ applying equation (6) with the $\delta^{18}O$ values from *Farquhar et al.* [1993].

[43] To our knowledge, there are no data for equilibrium (α_{eq}) and kinetic α_k isotopic fractionation of ^{17}O between liquid and gaseous water, nor have the ^{17}O partition coef-

ficients been determined. By scaling results for the diffusion coefficient of $H_2{}^{16}O$, $H_2{}^{18}O$, and $HD^{16}O$ [*Merlivat*, 1978] to $H_2{}^{17}O$, we calculate $^{17}\varepsilon_k$ of 13.7‰ from $^{18}\varepsilon_k$ of 26.5‰ [*Farquhar et al.*, 1989]. The isotopic ratios in precipitation water result from kinetic and equilibrium fractionations [*Craig and Gordon*, 1965]. On a global scale, equilibrium effects dominate. This is demonstrated by a model simulation by *Hendricks et al.* [2000], which is able to simulate precipitation isotope ratios with equilibrium fractionation alone. Applying equation (6) with a γ for precipitation water found by *Li and Meijer* [1998], we calculate $^{17}\alpha_{eq}$ from the equilibrium fractionation effect for $\delta^{18}O$ of 9.15‰ (25°C) [*Bottinga and Craig*, 1969]. We now have all the terms required to calculate $^{x}R_E$ for leaf water from equation (18).

[44] The reader should note that α_{lp} does not have any simple physical significance. The α_{lp} conflates the heavy isotope depletion of meteoric water with the heavy isotope enrichment of leaf water with respect to precipitation. It is not a general expression but applies only to the global average. The ratio of isotope effects $^{17}\varepsilon_{lp}/^{18}\varepsilon_{lp}$ is close to 0.5 but is actually dependent on the strength of individual processes in equation (18). The reason is that the ratio of isotope effects for meteoric water (precipitation and atmospheric water vapor) is different from the ratios for leaf water enrichment.

[45] We estimate gross O_2 production by the land biosphere starting with the gross carbon production value of 9.4×10^{15} mol C yr^{-1} (113 Gt C yr^{-1}) calculated from the Simple Biosphere 2 (Sib2) biosphere model [*Zhang et al.*, 1996]. We partition production between C3 plants (accounting for 72.5% of gross carbon production [*François et al.*, 1998]), which cycle additional carbon and oxygen by photorespiration, and C4 plants, which do not photorespire. Fluxes from C3 and C4 plants have to be scaled to a value for gross O_2 production by accounting for the relationship between O_2 and carbon production. We assume a photosynthetic quotient of 1.07 mol O_2 (mol C)$^{-1}$ for both C3 and C4 plants [*Keeling*, 1988]. We also assume that 10% of all O_2 production is consumed by the Mehler reaction.

[46] Taking the photosynthetic quotient and the Mehler reaction into account, O_2 production by C4 plants calculates to

$$3.1 \times 10^{15}\left(\mathrm{mol\,O_2\,yr^{-1}}\right) = 9.4 \times 10^{15}\left(\mathrm{mol\,C\,yr^{-1}}\right) \times 0.275 \times 1.07 \times \left(\mathrm{mol\,O_2\,(mol\,C)^{-1}}\right) \times 0.9^{-1}.$$

For C3 plants we have to include O_2 production associated with the production of organic carbon that is consumed by photorespiration. Equation (A9) of *von Caemmerer and Farquhar* [1981] expresses the photosynthetic electron transport rate, J_a, in C3 plants as a function of gross carbon production, the internal pCO_2 of leaves, and the compensation pCO_2. Since four electrons are transferred to fix one carbon, $J_a/4$ is the ratio of gross O_2 production including photorespiration to gross O_2 production estimated by Sib2. This ratio calculates to 1.99 using the following values for parameters in J_a. The compensation pCO_2 is taken as 34 ppmv [*Farquhar et al.*, 1980]. Thus the internal pCO_2 becomes 182 ppmv, assuming a preindustrial pCO_2 of 280 ppmv and a leaf pCO_2 to atmospheric pCO_2 ratio of 0.65. The latter term is calculated from the $\delta^{13}C$ of C3 plants [*Evans et al.*, 1986], assuming a discrimination of 18.9‰.

Table 1. Fractionation Factor for Terrestrial Respiration[a]

	Per Mil	Holocene Contribution	Glacial Contribution
Dark respiration	18.0‰	52%	47%
Photorespiration	21.2‰	38%	43%
Mehler reaction	15.1‰	10%	10%
Total respiration, $^{18}\varepsilon_{lr}$		18.913‰	19.087‰

[a] The $\delta^{18}O$ of O_2 fractionation by terrestrial respiration in the Holocene and the Last Glacial. Contributions from dark respiration, photorespiration, and Mehler reaction are calculated according to the calculation of the total oxygen flux for the terrestrial biosphere (see text). Fractionation factors are from *Guy et al.* [1992, 1993].

[47] Including the photosynthetic quotient and the Mehler reaction, the total O_2 production by C3 plants on land calculates to

$$1.6 \times 10^{16}\left(\mathrm{mol\,O_2\,yr^{-1}}\right) = 9.4 \times 10^{15}\left(\mathrm{mol\,C\,yr^{-1}}\right) \times 0.725 \times 1.99 \times 1.07\left(\mathrm{mol\,O_2(mol\,C)^{-1}}\right) \times 0.9^{-1}$$

Summed C3 and C4 gross O_2 production by the land biosphere, accounting for gross carbon production, photosynthetic quotient, photorespiration in C3 plants, and the Mehler reaction, is then 1.9×10^{16} mol yr^{-1}.

[48] The fractionation for land respiration $^{x}\alpha_{lr}$ incorporates contributions from dark respiration, photorespiration, and the Mehler reaction, each of which has a different fractionation factor. We calculate $^{18}\alpha_{lr}$ by scaling fractionations for the three respiration types [*Guy et al.*, 1992, 1993] according to their contributions in the calculation of gross oxygen production above (Table 1), and obtain $^{18}\varepsilon_{lr}$ of 18.9‰. As for ocean respiration, we calculate $^{17}\alpha_{lr}$ for land respiration applying equation (4) with a λ of 0.518 (see section 5.1.1).

5.1.3. Stratosphere

[49] F_{str} is the oxygen exchange flux between the stratosphere and the troposphere. We describe the stratospheric processes with a simple approach. Oxygen is transferred to the stratosphere without fractionation. O_2 in air reentering the troposphere is then fractionated by α_{str}. Note that α_{str} is a model parameter that has no simple physical significance. Its low value results from parameterizing the stratosphere as one box in our model. The α_{str} reflects the product of several isotope exchange reactions in the stratosphere scaled by the small fraction of O_2 exchanging with CO_2. For the stratosphere-atmosphere exchange flux we adopt the value from *Appenzeller et al.* [1996] of 4.9×10^{18} mol O_2 yr^{-1} through the 380°K isentropic surface.

[50] Isotope data for $\delta^{18}O$ and $\delta^{17}O$ of CO_2 in the troposphere and stratosphere show that stratospheric photochemistry fractionates ^{17}O up to twice as much as ^{18}O [*Thiemens et al.*, 1991, 1995a, 1995b; *Zipf and Erdman*, 1994]. Sparse data indicate that stratospheric samples below ~35 km are fractionated equally in ^{17}O and ^{18}O [*Thiemens et al.*, 1995a]. The isotope exchange between CO_2 and O_2 for oxygen reintroduced into the troposphere likely takes place in this lower stratospheric zone. Therefore we assume that the stratospheric fractionation factor is the same for ^{18}O and ^{17}O in our model. The value of stratospheric fractionation α_{str} will be determined by the model initialization.

Table 2. Model Parameters[a]

Variable	Description	^{18}O	^{17}O
$\varepsilon*$	equilibrium fractionation between dissolved and atmospheric O_2 [*Benson and Krause*, 1984]	0.700‰	0.381‰
ε_{ors}	mean fractionation during respiration in the marine mixed layer [*Kiddon et al.*, 1993]	−20.000‰	−10.410‰
ε_{ord}	mean fractionation during decomposition of organic carbon in the ocean interior [*Bender et al.*, 1994]	−12.000‰	−6.234‰
ε_{lr}	mean fractionation during terrestrial respiration (see Table 1)	−18.913‰	−9.842‰
ε_k	kinetic isotope fractionation between liquid and gaseous water [*Farquhar et al.*, 1989]	26.500‰	13.749‰
ε_{eq}	equilibrium isotope fractionation between liquid and gaseous water [*Bottinga and Craig*, 1969]	9.150‰	4.822‰
ε_{str}	fractionation in the stratosphere	-2.764×10^{-3}‰	-2.764×10^{-3}‰
ε_{lp}	leaf water enrichment (summarized fractionation of water cycle effects for terrestrial photosynthesis)	7.219‰	3.694‰
ε_S	GPP-weighted precipitation water versus standard mean ocean water (SMOW) [*Farquhar et al.*, 1993]	−7.900‰	−4.180‰
ε_V	GPP-weighted precipitation water vapor versus SMOW [*Farquhar et al.*, 1993]	−18.200‰	−9.653‰
R_{sw}	isotope ratio of seawater for SMOW [*Hoefs*, 1997]	2.00520×10^{-3}	3.73000×10^{-4}
R_{atm}	isotope ratio of atmospheric O_2 (calculated; see text)	2.05232×10^{-3}	3.77421×10^{-4}
F_{op}	gross photosynthetic oxygen flux from the ocean biosphere (see text for details)	1.09×10^{16} mol O_2 yr^{-1}	
F_{ors}	mixed layer respiration	0.95 F_{op}	
F_{ord}	deep ocean respiration	0.05 F_{op}	
F_{lp}	gross photosynthetic oxygen flux from the land biosphere (see text for details)	1.9×10^{16} mol O_2 yr^{-1}	
F_{str}	stratosphere-troposphere oxygen exchange flux [*Appenzeller et al.*, 1996]	4.9×10^{18} mol O_2 yr^{-1}	
	atmosphere versus SMOW [*Kroopnick and Craig*, 1972]	23.50‰	11.852‰

[a] Fractionation factors give ε values instead of α values used for model calculations $\alpha = (\varepsilon - 1)1000$. GPP is gross primary product. Leaf water enrichment, α_{lp}, and stratospheric fractionation, α_{str}, result from the initialization of our box model. References refer to the ^{18}O values. See text for the calculations of values for ^{17}O from ^{18}O values.

[51] We assume steady state, justified by the general stability of biogeochemical cycles during the ∼1.2 kyr lifetime of oxygen in the atmosphere. We solve equations (15) and (18), obtaining

$$ {}^{x}R_{atm} = \frac{\left[F_{lp}(1-h)\,{}^{x}\alpha_k\,{}^{x}R_S + h\,{}^{x}R_V\right]{}^{x}\alpha_{eq} + F_{op}\,{}^{x}R_{sw}}{F_{lr}\,{}^{x}\alpha_{1r} + F_{ors}\,{}^{x}\alpha_*\,{}^{x}\alpha_{ors} + F_{ord}\,{}^{x}\alpha_*\,{}^{x}\alpha_{ord} + F_{str}(1 - {}^{x}\alpha_{str})}. \quad (19) $$

[52] Equation (19) expresses the $^{17}O/^{16}O$ and $^{18}O/^{16}O$ ratios of O_2, and hence $\delta^{17}O$ and $\delta^{18}O$ of O_2, as a function of the following terms: the rates of land and ocean photosynthesis, the flux of O_2 in and out of the stratosphere, the isotopic composition of ocean water (equal to SMOW), the isotope fractionation factors described in the previous section, mean atmospheric humidity, and the model-based stratospheric oxygen fractionation factor. The definition of $\Delta^{17}O$ (equation (7)) in terms of isotopic ratios is

$$ \Delta^{17}O(\text{per meg}) = \left[\left(\frac{{}^{17}R_{atm}}{{}^{17}R_{atm0}} - 1\right) - 0.521\left(\frac{{}^{18}R_{atm}}{{}^{18}R_{atm0}} - 1\right)\right]10^6, \quad (20) $$

where ${}^{x}R_{atm0}$ are ratios of today's atmosphere. Using equations (20) and (19) for ^{18}O and ^{17}O, we can calculate $\Delta^{17}O$ for various combinations of ocean and land oxygen fluxes.

5.2. Initialization

[53] The model is initialized with fluxes and fractionation factors representing the preindustrial Earth. We assume that O_2 fluxes for the land, ocean, and stratospheric cycles are in steady state, meaning that $F_{lr} = F_{lp}$ and $F_{ors} + F_{ord} = F_{op}$.

[54] In equation (19) for ${}^{18}R_{atm}$ and ${}^{17}R_{atm}$, we have not specified values for h or α_{str}. With modern values for ${}^{18}R_{atm}$ and ${}^{17}R_{atm}$, equation (19) represents a problem with two equations and two unknowns, h and α_{str}. We calculate ${}^{18}R_{atm}$ and ${}^{17}R_{atm}$ from the current atmospheric $\delta^{18}O$ value of 23.50‰ versus SMOW [*Kroopnick and Craig*, 1972], from the $\Delta^{17}O$ of 249 per meg for seawater versus atmosphere [*Luz and Barkan*, 2000], and from the isotope ratios for SMOW reported by *Hoefs* [1997]. Table 2 lists values used for and resulting from the initialization.

[55] The stratospheric exchange reaction has a small effect on $\delta^{18}O$ (or $\delta^{17}O$) of atmospheric air, ∼0.4‰ [*Bender et al.*, 1994]. Since stratospheric fractionation is not very important in determining atmospheric $\delta^{18}O$ and $\delta^{17}O$, the term F_{str} $(1 - \alpha_{str})$ essentially drops out of equation (19), and the ratio of ocean to land productivity is much more important than α_{str} for constraining humidity h.

[56] The atmospheric $\Delta^{17}O$ value, 0 by definition for the initialization, basically results from a balance between biological oxygen fluxes with a positive $\Delta^{17}O$ and the stratospheric oxygen flux with a negative $\Delta^{17}O$. Thus the ratio of the stratospheric to the total biospheric oxygen flux essentially defines the stratospheric fractionation factor α_{str}.

[57] The initialization results in h = 55% and ${}^{18}\varepsilon_{lp}$ = 7.2‰. This is at the upper end of the estimates for the leaf water enrichment [*Farquhar et al.*, 1993; *Yakir et al.*, 1994] but is not unexpected [*Bender et al.*, 1994]. The ${}^{18}\varepsilon_{str}$ calculates to -2.8×10^{-3}‰ from our model initialization.

Table 3. Mean Values for Designated Time Periods[a]

	Period, ka BP	$\Delta^{17}O$, per meg	CO_2, ppmv	$\delta^{18}O_{sw}$, ‰ (SMOW)	$\delta^{18}O_{atm}$, ‰ (atm)
Modern	0	0	281	0.00	0.00
Late Holocene	0–5	−1	278	0.00	−0.03
Early Holocene	5–12.5	3	265	0.13	0.01
Transition	12.5–16	22	240	0.58	1.02
LGM	16–24	38	202	1.00	1.00
Midglacial	42–60	30	207	0.73	0.45

[a] Values used for model calculations. Initialization was made with the preanthropogenic value of atmospheric CO_2. This introduces an error of <3 per meg in the calculations (see text). Atmospheric $\delta^{18}O$ values ($\delta^{18}O_{atm}$ versus modern atmosphere) were taken from the GISP2 core [*Bender et al.*, 1999]. To obtain $\delta^{18}O_{sw}$ values, we scaled results from the core V19-30 [*Shackleton*, 1987] to a recent result from ocean water stored as pore fluids of the ocean floor, which gives a value of 1‰ for the last glacial maximum (LGM) [*Schrag et al.*, 1996].

[58] The steady state assumption neglects the stratospheric ozone decrease of the last few decades [*Kiehl et al.*, 1999; *Solomon*, 1999] and neglects the CO_2 increase since the beginning of the industrialization [*Barnola*, 1999]. Both are important in the stratospheric oxygen exchange reactions (equations (10), (11), (12), and (13)). However, the significance of the decadal to centennial changes for $\Delta^{17}O$ has to be considered in the context of the ~1200-year lifetime of atmospheric oxygen. Neglecting the anthropogenic ozone decrease introduces an error of <1 per meg in the atmospheric $\Delta^{17}O$ value. We estimate that keeping all other parameters constant, the anthropogenic CO_2 increase has led to a decrease of $\Delta^{17}O$ on the order of 3 per meg since preanthropogenic times. We cannot detect such a change with our record.

[59] We use our model to calculate the biological productivity during the four time periods highlighted in the ice core record (Figure 1), the midglacial (60–42 ka), the LGM (24–16 ka), the middle of the last glacial termination (16–12.5 ka), and the early Holocene (12.5–5 ka); mean $\Delta^{17}O$ values for these periods are +30, +38, +22, and +3 per meg, respectively (Table 3).

6. Model Results

[60] From the initialization process outlined in section 5.2, we know all fractionation factors and h (average humidity). From equations (19) and (20), we derive an equation that describes Oc, the fraction of the initial, modern ocean productivity, as a function of Ld, the fraction of the initial, modern land productivity, for constant $\Delta^{17}O$, fractionation factors, and the isotope ratios of seawater. This equation thus describes all possible combinations of Oc and Ld consistent with a particular value of $\Delta^{17}O$. Trivially, we can also describe the fraction of the modern total productivity as a function of Ld for a constant $\Delta^{17}O$.

6.1. Modern Case

[61] The thin solid lines in Figure 3 show the results of such a calculations for the "modern" case. The x axis is land production, the y axis of the top panel is ocean production, and the y axis of the bottom panel is total production, all expressed as percent of the modern value. The thin solid line in the top panel shows the variation in ocean production as land production changes, with $\Delta^{17}O$ held constant at the modern value of zero. Ocean productivity varies inversely with land productivity, because $\Delta^{17}O$ is quite insensitive to the relative magnitudes of these fluxes, but is mainly determined by the total O_2 productivity. Two effects define the slope of the isolines for ocean versus land productivity. First, the ratio of land to ocean fluxes used for the initialization of the box model is important, as this ratio determines h. Second, $\Delta^{17}O$ of O_2 produced by terrestrial photosynthesis is slightly less than that produced by oceanic photosynthesis. This second effect is also responsible for a slight dependence of the total productivity on the contribution from land and ocean cycles.

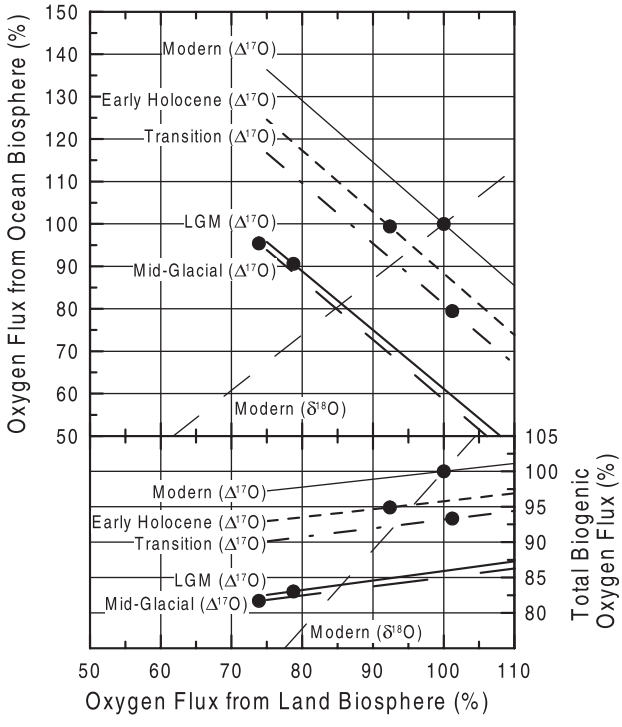

Figure 3. Estimates for total biogenic oxygen fluxes and individual contributions from land and ocean biospheres in percent relative to modern. Top panel shows relative contributions for land and ocean biosphere; bottom panel shows total biospheric oxygen flux versus land oxygen flux. Thin solid lines are isolines of constant $\Delta^{17}O$ for modern day. Thick lines are isolines of constant $\Delta^{17}O$ for mean values over the time periods designated in Figure 1. Thin dashed lines are isolines of constant $\delta^{18}O$ for modern. Dots are intersections of the $\Delta^{17}O$ and $\delta^{18}O$ isolines (only the modern $\delta^{18}O$ isoline is shown).

For a 10% change in land productivity the total productivity changes by ~1%. The modern curves in both panels of Figure 3, of course, pass through the points where land production equals 100% of modern and ocean and total production equal 100% of modern.

[62] We can also derive a function from equation (19) that describes all possible combinations of Oc and Ld consistent with given values of $\delta^{18}O$. The thin dashed line in Figure 3 shows this solution for the modern Earth. The $\delta^{18}O$ of O_2 constrains relative rates of terrestrial and marine production independent of the absolute rate of total global oxygen production by the biosphere. It thus contrasts with $\Delta^{17}O$ of O_2, which primarily reflects the total rate of oxygen production by the biosphere. For the $\delta^{18}O$ constraint the slope of the isoline is positive. As the absolute magnitude of the flux from the terrestrial biosphere increases, the flux from the marine biosphere must increase in order to maintain a constant $\delta^{18}O$. The overall solution for the modern climate, in accordance with both $\delta^{18}O$ and $\Delta^{17}O$, is given by the intercept of the thin solid line and the thin dashed line. Trivially, for the modern initialization case the intercept is at 100% of modern land and ocean production and at 100% of modern total production.

6.2. Solutions for Past Time Periods

[63] We now examine the solutions for the time periods designated in Figure 1. For these time periods we have to make slight adjustments to the stratospheric fractionation factor, the fractionation factor for land respiration, the isotopic composition of seawater, and the isotopic composition of the atmosphere (for $\delta^{18}O$ isolines).

[64] The isotopic composition of ocean water between glacial and interglacial periods varies because of changes in the amount of isotopically lighter water stored in continental ice sheets (Table 3). This water has undergone fractionation with the signature of precipitation water. We adopt $\delta^{18}O$ values of benthic foraminifera from the deep-sea core V19-30 [*Shackleton*, 1987] as a record of relative changes in $\delta^{18}O_{sw}$ versus time. We scale this record to an amplitude of 1‰ for the deglacial change in $\delta^{18}O_{sw}$ based on studies of pore fluids in seafloor sediments [*Schrag et al.*, 1996]. We calculate values of $\delta^{17}O_{sw}$ from $\delta^{18}O_{sw}$ assuming that the relationship between $\delta^{18}O$ and $\delta^{17}O$ of water deposited on the ice sheets follows equation (6) with a γ of 0.528 [*Li and Meijer*, 1998]. For the atmospheric $\delta^{18}O$ of O_2 values for specified periods, we take results from the GISP2 ice core [*Bender et al.*, 1999] (Table 3).

[65] Oxygen isotope fractionation for terrestrial respiration also varies between glacial and interglacial times. During glacial times the atmospheric CO_2 concentration is lower, and C3 plants consume a greater fraction of gross O_2 production by photorespiration. On the other hand, we expect that more photosynthesis during the ice age comes from C4 plants [*Collatz et al.*, 1998; *François et al.*, 1998; *Street-Perrott et al.*, 1997], which do not photorespire.

[66] *François et al.* [1998] calculate that the contribution of C4 plants to net primary carbon productivity decreases from 39.0% in the glacial to 27.5% in interglacial periods. The net effect is that the contribution of photorespiration rises from 38% of total respiration at present to 43% in the glacial (Table 1). The respiratory isotope effect of land respiration on $\delta^{18}O$ changes from -18.9‰ today to -19.1‰ in the glacial. We assume that LGM numbers apply to the midglacial and LGM time slices and that modern numbers apply to all the other time slices.

[67] We scale α_{str} for the different CO_2 levels during the preanthropogenic time periods but make no adjustment for variations in ozone levels in the stratosphere. Modeling studies suggest that the stratospheric ozone level has been surprisingly stable from the last glacial to the preindustrial Holocene [*Crutzen and Brühl*, 1993; *Martinerie et al.*, 1995]. Annual mean insolation has changed little between glacial and interglacial. This, together with the unchanged ozone concentration, suggests that the ozone photolysis rate has been constant as well. These models do not calculate the isotopic compositions of ozone. The magnitude of the ozone isotope fractionation is temperature dependent [*Krankowsky et al.*, 2000]. Models calculate a stratospheric temperature decrease from the LGM to the preindustrial Holocene [*Crutzen and Brühl*, 1993; *Martinerie et al.*, 1995] of ~4°C at 30 km altitude. *Krankowsky et al.* [2000] observe an increased isotopic fractionation of $\delta^{18}O$ of ozone by ~2% for a 4°C temperature increase. Fractionation of $\delta^{17}O$ of O_2 presumably increases by the same ratio. In our model this change is represented by a similar increase in $^{17}\alpha_{str}$ and $^{18}\alpha_{str}$. For a given value of land production, total production increases by ~2%, and ocean production increases by ~4%, compared to the initial LGM values. We note the effect and its magnitude but do not account for it in the ensuing discussion.

[68] We can now begin discussing results of our paleoproductivity calculations. First, consider solutions for $\Delta^{17}O$ alone. In Figure 3 these solutions are denoted by the thick solid lines. At any particular value for land productivity, we see a steady increase in total oxygen production from the glacial to the preanthropogenic Holocene (Figure 3, bottom panel). Midglacial and LGM O_2 productivities were ~15% lower than at present. The deglacial transition, roughly corresponding to the Bølling/Allerød period, saw oxygen productivities ~7% lower than today. The early Holocene probably still experienced oxygen productivities a few percent lower than today. The bottom panel in Figure 3 shows that these values are fairly insensitive to the assumed contribution of land (or ocean) photosynthesis to the total.

[69] Mean $\Delta^{17}O$ values for the last glacial maximum are 8 per meg lower than for the midglacial. Despite this significant difference in $\Delta^{17}O$, isolines for ocean productivity and total productivity versus land productivity are very similar. The change in $\Delta^{17}O$ between these periods results from a change in the CO_2 concentration. Productivity remained nearly constant.

[70] We next look at Oc and Ld values for the various periods calculated from the intersections of $\Delta^{17}O$ and $\delta^{18}O$ isolines. First, we consider uncertainties associated with these two isotope constraints. Our view is that $\Delta^{17}O$ poses a robust constraint on total production, but $\delta^{18}O$ does not give a robust constraint on ocean/land production. We therefore believe that the triple isotope composition of O_2 during the LGM gives a robust constraint on the fertility of the biosphere but does not give useful estimates of the individ-

ual productivities of the two realms without additional information.

[71] We are confident in our total production estimates because anomalous O_2 isotope fractionation in the stratosphere is very different from normal O_2 isotope fractionation by biological processes. Important details of stratospheric isotope exchange remain to be understood. However, experimental and modeling results make it very unlikely that the CO_2-O_2 exchange differed much during the past, except due to atmospheric CO_2 changes. In contrast, we cannot close the ^{18}O mass balance of O_2 [*Bender et al.*, 1994], because we have not been able to adequately quantify the complicated and diverse hydrological and biological O_2 isotope fractionation. For example, the $\delta^{18}O$ of leaf water is highly variable and may differ from the Craig equation [e.g., *White*, 1989], even under laboratory conditions [*Yakir et al.*, 1994]. Another example is that O_2 isotope fractionation by marine organisms is not well understood, either in the dark [*Kiddon et al.*, 1993] or in the light [e.g., *Quay*, 1997]. There is a large isotope effect associated with the alternative pathway of respiration [*Guy et al.*, 1993], but the importance of this pathway remains unquantified. *Angert et al.* [2001] have shown that soil respiration attenuates the ^{18}O enrichment associated with land respiration; again, the magnitude is unquantified.

[72] Nevertheless, we temporarily retain the $\delta^{18}O$ constraint, and use it together with the $\Delta^{17}O$ constraint, to calculate O_2 production by the land and ocean biosphere during our time slices. For reasons indicated above, we have strong confidence in the land plus ocean gross production but have little confidence in the land to ocean partitioning.

[73] For the LGM the combined $\Delta^{17}O$ and $\delta^{18}O$ results produce a solution (Figure 3, the solid circle on the thick heavy line) with a total O_2 productivity equal to 83% of today's value. According to the two isotopic constraints the ocean and the land productivity were both lower than at present. The O_2 flux from the land biosphere was 79% of the modern land flux, and the O_2 flux from the ocean was 91% of the modern ocean flux. The solution for midglacial suggests a slightly lower total biogenic oxygen flux, higher oceanic contribution, and lower land contribution. This is due to the lower Dole effect during the midglacial compared to the LGM.

[74] Over the transition a 20% reduction in ocean productivity versus today is suggested, but the calculation of this number is problematic. The $\delta^{18}O$ approach is sensitive to the value of the Dole effect, the difference in $\delta^{18}O$ between atmospheric oxygen and mean ocean water. The magnitude of the Dole effect during the glacial termination is difficult to interpret. The Dole effect is interpreted as a steady state feature. However, transient terms associated with the changing $\delta^{18}O$ of seawater, and the influence of isotopically light meltwater on the isotopic composition of surface ocean water and precipitation, were important during the deglaciation. Furthermore, $\delta^{18}O$ values from atmospheric O_2 are obtained from ice core records and $\delta^{18}O$ values for ocean water are obtained from deep see cores. These records from different climate archives have to be properly synchronized. Over the transition the data we use indicate a relatively high Dole effect (see Table 3), which could partly result from uncertainties in the dating of the two records. Reducing the high Dole effect to the modern value over the transition leads to higher ocean productivity reaching 90%.

[75] According to the combined $\delta^{18}O$ and $\Delta^{17}O$ constraints, total biogenic O_2 production during the early Holocene was slightly lower than today. The ocean contribution was similar to today's level, while the land contribution was ~92% of the present value. A summary of our results for the total biogenic oxygen flux over time is displayed together with other climate records in Figure 4.

6.3. Last Glacial Maximum

[76] How do our results for the LGM compare to other estimates for the land productivity at this time? The range of estimates is large. We compare our results to a preliminary result of the latest version of the global biome model (BIOME), which calculates LGM terrestrial gross productivity at ~45% of modern (J. Kaplan and I. C. Prentice, personal communication, 1999). In another work, *François et al.* [1998] use the Carbon Assimilation In the Biosphere (CARAIB) model to estimate glacial terrestrial net primary productivity at 71% of modern.

[77] In order to make the comparison, we convert these model estimates for carbon productivities to gross oxygen productivities. We calculate gross oxygen productivity from gross carbon productivity similarly to our calculation for the modern fluxes, taking into account the shift from C3 to C4 plants in the glacial [*François et al.*, 1998] and increased photorespiration corresponding to lower CO_2 of ~200 ppmv compared to the initialization. For the CARAIB result we assume that gross primary productivity changed in parallel with net primary productivity. We obtain 50 and 80% gross oxygen flux from the terrestrial biosphere in the glacial compared to the present for the BIOME and CARAIB model results, respectively.

[78] The intercept of the $\Delta^{17}O$ and $\delta^{18}O$ solutions for the LGM in our calculation is ~80% land productivity and compares well to the CARAIB model estimate. However, this agreement should not be interpreted as proof for the higher estimate. We assumed for our model calculation that all fractionation factors remained constant in the past. This is questionable, especially for the LGM. Recently, a model simulation by G. Hoffmann (personal communication, 2001) shows that the global average fractionation factor for leaf water enrichment may have been higher during the glacial period. This is due to a larger relative contribution from low-latitude vegetation to the terrestrial biosphere O_2 flux as land productivity at higher latitudes was decreased. Increasing the leaf water enrichment for the glacial period changes the model results for both $\delta^{18}O$ and $\Delta^{17}O$ by affecting the isotopic ratio of O_2 produced by terrestrial photosynthesis. The effect is large for the $\delta^{18}O$ isoline but is relatively small for the $\Delta^{17}O$ isoline. A higher leaf water enrichment (ε_{lp}) for the LGM basically shifts the intersection of the $\delta^{18}O$ and $\Delta^{17}O$ isolines toward lower land and higher ocean contributions. On the $\Delta^{17}O$ LGM isolines, 50% land productivity, calculated for the BIOME model result, corresponds to 130% ocean and 79% total productivity relative to modern (see Figure 5). However, increasing the leaf

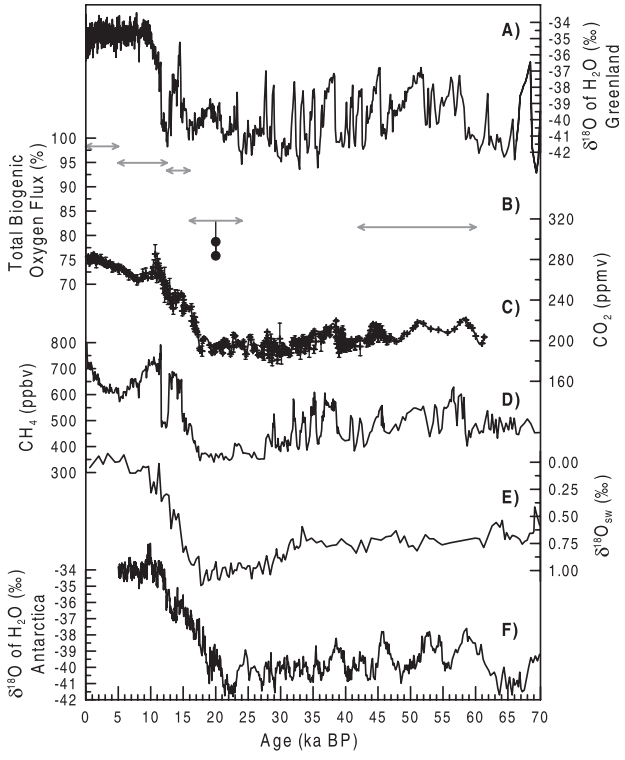

Figure 4. Total biospheric productivity versus time plotted together with other climate records. The $\delta^{18}O$ of the ice, a proxy for local temperature (a) from the GISP2 ice core, Greenland [*Grootes et al.*, 1993] and (f) from the Byrd ice core, Antarctica [*Johnsen et al.*, 1972]. (b) Total biospheric productivity calculated from $\Delta^{17}O$ and $\delta^{18}O$. Shaded arrows are estimates of the total biospheric productivity from Figure 3. Dots bound the estimates of total biogenic productivity for a land productivity of 50% modern (see Figure 5 and section 6.3). Solid line is the range of total productivity for a land productivity at 50–80% of modern (see section 6.3 for details). (c) Composite record of atmospheric CO_2 from Byrd station and Taylor Dome ice cores, Antarctica [*Indermühle et al.*, 2000; *Indermühle*, 1999; *Stauffer et al.*, 1998]. (d) Composite record of atmospheric CH_4 from Greenland Ice Core Project (GRIP) and GISP2 ice cores, Greenland [*Blunier and Brook*, 2001]. Ice core results ($\delta^{18}O$, CH_4, and CO_2) from Byrd and GRIP are plotted on the GISP2 timescale [*Blunier and Brook*, 2001]. Timescale for the glacial Taylor Dome CO_2 record from *Indermühle et al.* [2000] (Vostok GT4) has been adjusted to the GISP2 timescale so that the relative position of CO_2 and Antarctic temperature variations is preserved. (e) Relative changes in $\delta^{18}O_{sw}$ versus time. The $\delta^{18}O$ values of benthic foraminifera from the deep-sea core V19-30 [*Shackleton*, 1987] have been scaled to an amplitude of 1‰ based on a study of pore fluids in seafloor sediments [*Schrag et al.*, 1996]. The ^{14}C timescale of this deep-sea record has been converted to calendar ages using the calibration curve by *Bard et al.* [1993].

water enrichment has some consequences for our calculations that we will now explore in detail.

[79] According to equation (18) the leaf water enrichment can be increased in two ways: (1) by decreasing global gross primary product (GPP) weighted humidity and (2) by increasing the $\delta^{17}O$ and $\delta^{18}O$ of the global GPP-weighted precipitation. The two approaches weight contributions from equilibrium and kinetic fractionations differently, and the solutions for the two approaches differ slightly. We first consider the scenario where humidity is decreased. In Figure 5 the thin solid line marks the intersections of $\delta^{17}O$ and $\delta^{18}O$ isolines for decreasing humidity (monotonically increasing leaf water enrichment). This line starts at the original LGM solution (open diamond) on the original $\Delta^{17}O$ isoline (thick solid line). The solution at 50% of modern terrestrial O_2 productivity is found when relative humidity is 45%. In a second scenario, where leaf water

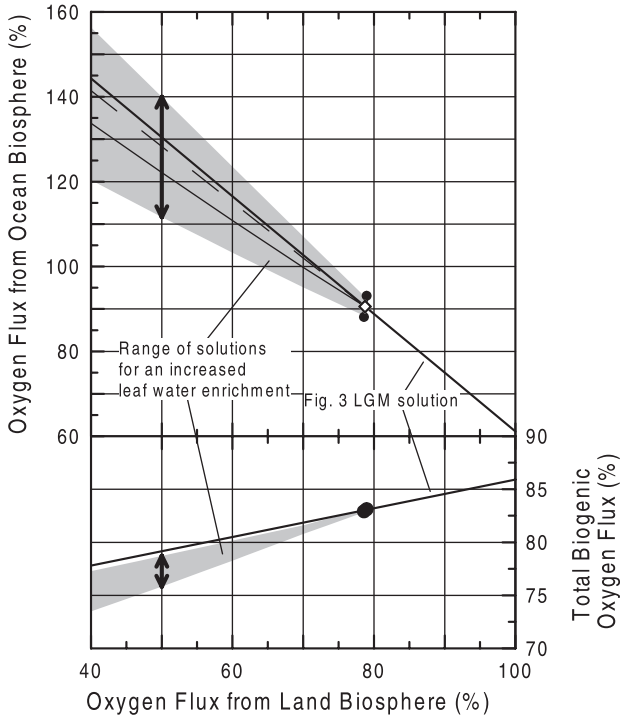

Figure 5. Same as Figure 3 but showing different estimates for the LGM. Thick solid lines and open diamond are identical to the LGM $\Delta^{17}O$ isolines and the intersection of $\Delta^{17}O$ and $\delta^{18}O$ isolines, respectively, in Figure 3. Dots on thick line show the range of solutions for the original LGM calculation, allowing variations of the initialization ratio of the land to ocean O_2 production of ±25%. Thin lines are defined by intersects of $\Delta^{17}O$ and $\delta^{18}O$ obtained with an increased isotope value of gross primary product weighted precipitation (thin dashed line) and decreased humidity (thin solid line). Shaded area is obtained by allowing a ±25% variation of the initialization ratio of the land to ocean O_2 production with increased leaf water enrichment. Vertical arrows show the range of suggested ocean and total productivities for the 50% land flux scenario suggested by a preliminary study from the BIOME model (J. Kaplan and I. C. Prentice, personal communication, 1999).

enrichment increases because of a higher isotopic ratio of GPP-weighted precipitation, we obtain the thin dashed line in Figure 5. At 50% modern land productivity, $\delta^{18}O$ is equal to −4.4‰, compared to −7.9‰ in the original LGM calculation.

[80] At these increased leaf water enrichments, calculated gross O_2 production is more sensitive to the initialization than in the previous formulation. In Figure 5 we give the range of solutions for the revised LGM solutions where the initialization land/ocean ratio is changed by ±25%. The shaded area is our best estimate of the range of solutions with an increased leaf water enrichment. If land productivity during the LGM was 50% of the present land productivity, as suggested by the BIOME model, ocean productivity increases to 111–140% of modern, while total productivity decreases to 76–79% of modern. In a similar fashion for the glacial termination, the particular values for the initialization ratio of terrestrial to marine O_2 production and the isotope enrichment of leaf water also influence the partitioning of production, while total productivity is barely affected.

[81] In summary, we use the estimates from the BIOME and CARAIB models (50% and 80%, respectively) as bounds for land productivity during the LGM. Between these estimates, our model results in a range of 88–140% of the modern oxygen flux for the ocean biosphere during the LGM. Even for such diverse estimates of land/ocean fluxes, the total oxygen flux is in the relatively small range of 76–83% of modern.

7. Conclusions

[82] The $\Delta^{17}O$ approach to global oxygen productivity gives, despite a large number of uncertainties, a robust estimate of the total global oxygen productivity in the past. We estimate that total biogenic productivity was ∼76–83% during the LGM as compared to today. A similar value is calculated for the midglacial. The glacial-interglacial transition, roughly corresponding to the Bølling/Allerød period, saw oxygen productivities ∼7% lower, and the early Holocene experienced oxygen productivities a few percent lower than today.

[83] Individual contributions of land and ocean biosphere are difficult to estimate because of uncertainties in the leaf water fractionation in the past and because of changes in modes of O_2 cycling. However, with estimates of land or ocean biosphere productivity we are able to give a good estimate of the other parameter. Biosphere models calculate that the land biosphere was much less fertile during the last glacial, but there is not good agreement between the quantitative estimates of the reduction. Given the wide range of these estimates (50–80%), we are only able to narrow the ocean productivity to 88–140% of the modern oxygen flux.

[84] Increased carbon uptake by the oceans must have overcompensated the reduction of the terrestrial carbon reservoir to explain the lower CO_2 concentrations in the glacial. Knowing the oceanic oxygen productivity is an important constraint for global carbon-cycle simulations. However, the interpretation of our results in terms of past atmospheric CO_2 changes awaits reliable estimates of the productivity of the terrestrial biosphere.

[85] **Acknowledgments.** This work was supported by the Swiss and the U.S. National Science Foundations. This work has particularly benefited from contributions of three colleagues. Boaz Luz (Hebrew University) shared with us his knowledge about the analysis of $\Delta^{17}O$ of O_2 and its alteration by biological processes. Joe Berry (Carnegie Institution of Washington) guided us in making a consistent calculation of gross O_2 production by the land biosphere, which we could not have done without his aid. Harro Meijer (Groningen University) offered important insight on the principles of triple isotope fractionation. We also thank Klaus Keller (Princeton University), Markus Leuenberger (University of Bern), Georg Hoffmann (Laboratoire des Sciences du Climat et de l'Environnement), and two thorough anonymous reviewers for discussion and comments. Any errors are our responsibility alone.

References

Angert, A., B. Luz, and D. Yakir, Fractionation of oxygen isotopes by respiration and diffusion in soils and its implications for the isotopic composition of atmospheric O_2, *Global Biogeochem. Cycles*, *15*, 871–881, 2001.

Appenzeller, C., J. R. Holton, and K. H. Rosenlof, Seasonal variation of mass transport across the tropopause, *J. Geophys. Res.*, *101*, 15,071–15,078, 1996.

Bard, E., M. Arnold, R. G. Fairbanks, and B. Hamelin, $^{230}Th-^{234}U$ and ^{14}C ages obtained by mass spectrometry on corals, *Radiocarbon*, *35*, 191–199, 1993.

Barnola, J. M., Status of the atmospheric CO_2 reconstruction from ice cores analyses, *Tellus, Ser. B*, *51*, 151–155, 1999.

Barth, V., and A. Zahn, Oxygen isotope composition of carbon dioxide in the middle atmosphere, *J. Geophys. Res.*, *102*, 12,995–13,007, 1997.

Bender, M. L., The $\delta^{18}O$ of dissolved O_2 in seawater: A unique tracer of circulation and respiration in the deep sea, *J. Geophys. Res.*, *95*, 22,243–22,252, 1990.

Bender, M., T. Sowers, and L. Labeyrie, The Dole effect and its variations during the last 130,000 years as measured in the Vostok ice core, *Global Biogeochem. Cycles*, *8*, 363–376, 1994.

Bender, M., J. Orchardo, M.-L. Dickson, R. Barber, and S. Lindley, In vitro O-2 fluxes compared with C-14 production and other rate terms during the JGOFS Equatorial Pacific experiment, *Deep Sea Res., Part I*, *46*, 637–654, 1999.

Bender, M. L., M.-L. Dickson, and J. Orchardo, Net and gross production in the Ross Sea as determined by incubation experiments and dissolved O-2 studies, *Deep Sea Res., Part II*, *47*, 3141–3158, 2000.

Benson, B. B., and D. Krause, The concentration and isotopic fractionation of oxygen dissolved in fresh-water and seawater in equilibrium with the atmosphere, *Limnol. Oceanogr.*, *29*, 620–632, 1984.

Blunier, T., and E. J. Brook, Timing of millennial-scale climate change in Antarctica and Greenland during the last glacial period, *Science*, *291*, 109–112, 2001.

Bottinga, Y., and H. Craig, Oxygen isotope fractionation between CO_2 and water, and the isotopic composition of marine atmospheric CO_2, *Earth Planet. Sci. Lett.*, *5*, 285–295, 1969.

Broecker, W. S., Ocean chemistry during glacial time, *Geochim. Cosmochim. Acta*, *46*, 1689–1705, 1982.

Collatz, G. J., J. A. Berry, and J. S. Clark, Effects of climate and atmospheric CO_2 partial pressure on the global distribution of C_4 grasses: Present, past and future, *Oecologia*, *114*, 441–454, 1998.

Cowling, S. A., and R. F. Sage, Interactive effects of low atmospheric CO_2 and elevated temperature on growth, photosynthesis and respiration in *Phaseolus vulgaris*, *Plant Cell Environ.*, *21*, 427–435, 1998.

Craig, H., and L. I. Gordon, Deuterium and oxygen 18 variations in the ocean and the marine atmosphere, in *Stable Isotopes in Oceanographic Studies and Paleotemperatures*, edited by E. Tongiorgi, p. 122, Cons. Naz. delle Ric., Lab. di Geol. Nucleare, Pisa, Italy, 1965.

Crutzen, P. J., and C. Brühl, A model study of atmospheric temperatures and the concentrations of ozone, hydroxyl, and some other photochemically active gases during the glacial, the preindustrial Holocene, and the present, *Geophys. Res. Lett.*, *20*, 1047–1050, 1993.

de Noblet, N. I., I. C. Prentice, S. Joussaume, D. Texier, A. Botta, and A. Haxeltine, Possible role of atmosphere–biosphere interactions in triggering the last glaciation, *Geophys. Res. Lett.*, *23*, 3191–3194, 1996.

Dickson, M.-L., J. Orchardo, R. T. Barber, J. Marra, J. J. McCarthy, and R. N. Sambrotto, Production and respiration rates in the Arabian Sea

during the 1995 Northeast and Southwest Monsoons, *Deep Sea Res., Part II*, *48*, 1199–1230, 2001.

Evans, J. R., T. D. Sharkey, J. A. Berry, and G. D. Farquhar, Carbon isotope discrimination measured concurrently with gas exchange to investigate CO_2 diffusion in leaves of higher plants, *Aust. J. Plant Physiol.*, *13*, 281–292, 1986.

Farquhar, G. D., S. von Caemmerer, and J. A. Berry, A biochemical-model of photosynthetic CO_2 assimilation in leaves of C-3 species, *Planta*, *149*, 78–90, 1980.

Farquhar, G. D., K. T. Hubick, A. G. Condon, and R. A. Richards, Carbon isotope fractionation and plant water-use efficiency, in *Stable Isotopes in Ecological Research*, edited by P. W. Rundel, J. R. Ehleringer, and K. A. Nagy, pp. 21–40, Springer-Verlag, New York, 1989.

Farquhar, G. D., J. Lloyd, J. A. Taylor, L. B. Flanagan, J. P. Syvertsen, K. T. Hubick, S. C. Wong, and J. R. Ehleringer, Vegetation effects on the isotope composition of oxygen in atmospheric CO_2, *Nature*, *363*, 439–442, 1993.

Field, C. B., M. J. Behrenfeld, J. T. Randerson, and P. Falkowski, Primary production of the biosphere: Integrating terrestrial and oceanic components, *Science*, *281*, 237–240, 1998.

François, L. M., C. Delire, P. Warnant, and G. Munhoven, Modelling the glacial-interglacial changes in the continental biosphere, *Global Planet. Change*, *17*, 37–52, 1998.

Fung, I. Y., S. K. Meyn, I. Tegen, S. C. Doney, J. G. John, and J. K. B. Bishop, Iron supply and demand in the upper ocean, *Global Biogeochem. Cycles*, *14*, 281–295, 2000.

Gallimore, R. G., and J. E. Kutzbach, Role of orbitally induced changes in tundra area in the onset of glaciation, *Nature*, *381*, 503–505, 1996.

Gamo, T., M. Tsutsumi, H. Sakai, T. Nakazawa, M. Tanaka, H. Honda, H. Kubo, and T. Itoh, Carbon and oxygen isotopic ratios of carbon dioxide of a stratospheric profile over Japan, *Tellus, Ser. B*, *41*, 133–187, 1989.

Gao, Y. Q., and R. A. Marcus, Strange and unconventional isotope effects in ozone formation, *Science*, *293*, 259–263, 2001.

Grootes, P. M., M. Stuiver, J. W. C. White, S. J. Johnsen, and J. Jouzel, Comparison of oxygen isotope records from the GISP2 and GRIP Greenland ice cores, *Nature*, *366*, 552–554, 1993.

Guy, R. D., J. A. Berry, M. L. Fogel, D. H. Turpin, and H. G. Weger, Fractionation of the stable isotopes of oxygen during respiration by plants: The basis of a new technique to estimate partitioning to the alternative path, in *Molecular, Biochemical and Physiological Aspects of Plant Respiration*, edited by H. Lambers and L. H. W. van der Plas, pp. 443–453, SPB Academic, The Hague, 1992.

Guy, R. D., M. L. Fogel, and J. A. Berry, Photosynthetic fractionation of the stable isotopes of oxygen and carbon, *Plant Physiol.*, *101*, 37–48, 1993.

Hendricks, M. B., D. J. DePaolo, and R. C. Cohen, Space and time variation of $\delta^{18}O$ and δD in precipitation: Can paleotemperature be estimated from ice cores?, *Global Biogeochem. Cycles*, *14*, 851–861, 2000.

Hoefs, J., *Stable Isotope Geochemistry*, 201 pp., Springer-Verlag, New York, 1997.

Hulston, J. R., and H. G. Thode, Variations in the S^{33}, S^{34}, and S^{36} contents of meteorites and their relation to chemical and nuclear effects, *J. Geophys. Res.*, *70*, 3475–3484, 1965.

Indermühle, A., Holocene carbon-cycle dynamics based on CO_2 trapped in ice at Taylor Dome, *Antarctica, Nature*, *398*, 121–126, 1999.

Indermühle, A., E. Monnin, B. Stauffer, T. F. Stocker, and M. Wahlen, Atmospheric CO_2 concentration from 60 to 20 kyr BP from the Taylor Dome ice core, *Antarctica, Geophys. Res. Lett.*, *27*, 735–738, 2000.

Johnsen, S. J., W. Dansgaard, H. B. Clausen, and C. C. Langway Jr., Oxygen isotope profiles through the Antarctic and Greenland ice sheets, *Nature*, *235*, 429–434, 1972.

Keeling, R. F., Development of an interferometric oxygen analyzer for precise measurement of the atmospheric O_2 mole fraction, doctoral thesis, Harvard Univ., Cambridge, Mass., 1988.

Kiddon, J., M. L. Bender, J. Orchardo, D. A. Caron, J. C. Goldman, and M. Dennett, Isotopic fractionation of oxygen by respiring marine organisms, *Global Biogeochem. Cycles*, *7*, 679–694, 1993.

Kiddon, J., M. L. Bender, and J. Marra, Production and respiration in the 1989 North Atlantic spring bloom: An analysis of irradiance-dependent changes, *Deep Sea Res., Part I*, *42*, 553–576, 1995.

Kiehl, J. T., T. L. Schneider, R. W. Portmann, and S. Solomon, Climate forcing due to tropospheric and stratospheric ozone, *J. Geophys. Res.*, *104*, 31,239–31,254, 1999.

Kleidon, A., K. Fraedrich, and M. Heimann, A green planet versus a desert world: Estimating the maximum effect of vegetation on the land surface climate, *Clim. Change*, *44*, 471–493, 2000.

Krankowsky, D., P. Lammerzahl, and K. Mauersberger, Isotopic measurements of stratospheric ozone, *Geophys. Res. Lett.*, *27*, 2593–2595, 2000.

Kroopnick, P. M., Oxygen 18 in dissolved oxygen, in *GEOSECS Atlantic, Pacific and Indian Ocean Expeditions: Shorebased Data and Graphics*, edited by H. G. Ostlund et al., pp. 3, 27-182, U. S. Gov. Print. Off., Washington, D. C., 1987.

Kroopnick, P., and H. Craig, Atmospheric oxygen: Isotopic composition and solubility fractionation, *Science*, *175*, 54–55, 1972.

Kroopnick, P., and H. Craig, Oxygen isotope fractionation in dissolved oxygen in deep-sea, *Earth Planet. Sci. Lett.*, *32*, 375–388, 1976.

Kutzbach, J. E., P. J. Bartlein, J. A. Foley, S. P. Harrison, S. W. Hostetler, Z. Liu, I. C. Prentice, and T. Webb, Potential role of vegetation feedback in the climate sensitivity of high-latitude regions: A case study at 6000 years BP, *Global Biogeochem. Cycles*, *10*, 727–736, 1996.

Lane, G. A., and M. Dole, Fractionation of oxygen isotopes during respiration, *Science*, *123*, 574–576, 1956.

Li, W. J., and H. A. J. Meijer, The use of electrolysis for accurate $\delta^{17}O$ and $\delta^{18}O$ isotope measurements in water, *Isot. Environ. Health Stud.*, *34*, 349–369, 1998.

Luz, B., and E. Barkan, Assessment of oceanic productivity with the triple-isotope composition of dissolved oxygen, *Science*, *288*, 2028–2031, 2000.

Luz, B., E. Barkan, M. L. Bender, M. H. Thiemens, and K. A. Boering, Triple-isotope composition of atmospheric oxygen as a tracer of biosphere productivity, *Nature*, *400*, 547–550, 1999.

Mahowald, N., K. Kohfeld, M. Hansson, Y. Balkanski, S. P. Harrison, I. C. Prentice, M. Schulz, and H. Rodhe, Dust sources and deposition during the last glacial maximum and current climate: A comparison of model results with paleodata from ice cores and marine sediments, *J. Geophys. Res.*, *104*, 15,895–15,916, 1999.

Martin, J. H., Glacial-interglacial CO_2 change: The iron hypothesis, *Paleoceanography*, *5*, 1–13, 1990.

Martinerie, P., G. P. Brasseur, and C. Granier, The chemical composition of ancient atmospheres: A model study constrained by ice core data, *J. Geophys. Res.*, *100*, 14,291–14,304, 1995.

Mauersberger, K., B. Erbacher, D. Krankowsky, J. Günther, and R. Nickel, Ozone isotope enrichment: Isotopomer-specific rate coefficients, *Science*, *283*, 370–372, 1999.

Merlivat, L., Molecular diffusivities of H_2O^{16}, $H_2{}^{16}O$ and $H_2{}^{18}O$ in gases, *J. Chem. Phys.*, *69*, 2864–2871, 1978.

Mook, W. G., *Environmental Isotopes in the Hydrological Cycle: Principles and Applications*, vol. I, *Introduction: Theory, Methods, Review*, Int. At. Energy Agency, U. N., Paris, 2000.

Quay, P., Was a carbon balance measured in the equatorial Pacific during JGOFS?, *Deep Sea Res., Part II*, *44*, 1765–1781, 1997.

Schrag, D. P., G. Hampt, and D. W. Murray, Pore fluid constraints on the temperature and oxygen isotopic composition of the glacial ocean, *Science*, *272*, 1930–1932, 1996.

Schwander, J., The transformation of snow to ice and the occlusion of gases, in *The Environmental Record in Glaciers and Ice Sheets*, edited by H. Oeschger and C. C. Langway Jr., pp. 53–67, John Wiley, New York, 1989.

Schwander, J., T. Sowers, J.-M. Barnola, T. Blunier, B. Malaizé, and A. Fuchs, Age scale of the air in the summit ice: Implication for glacial-interglacial temperature change, *J. Geophys. Res.*, *102*, 19,483–19,494, 1997.

Shackleton, N. J., Oxygen isotopes, ice volume and sea level, *Quat. Sci. Rev.*, *6*, 183–190, 1987.

Shackleton, N. J., The 100,000-year ice-age cycle identified and found to lag temperature, carbon dioxide and orbital eccentricity, *Science*, *289*, 1897–1902, 2000.

Sigman, D., and E. A. Boyle, Glacial/interglacial variations in atmospheric carbon dioxide, *Nature*, *407*, 859–869, 2000.

Solomon, S., Stratospheric ozone depletion: A review of concepts and history, *Rev. Geophys.*, *37*, 275–316, 1999.

Stauffer, B., et al., Atmospheric CO_2 concentration and millennial-scale climate change during the last glacial period, *Nature*, *392*, 59–62, 1998.

Street-Perrott, F. A., Y. S. Huang, R. A. Perrott, G. Eglinton, P. Barker, L. Ben Khelifa, D. D. Harkness, and D. O. Olago, Impact of lower atmospheric carbon dioxide on tropical mountain ecosystems, *Science*, *278*, 1422–1426, 1997.

Thiemens, M. H., Atmosphere science: Mass-independent isotope effects in planetary atmospheres and the early solar system, *Science*, *283*, 341–345, 1999.

Thiemens, M. H., T. Jackson, K. Mauersberger, B. Schueler, and J. Morton, Oxygen isotope fractionation in stratospheric CO_2, *Geophys. Res. Lett.*, *18*, 669–672, 1991.

Thiemens, M. H., T. Jackson, E. C. Zipf, P. W. Erdman, and C. Vanegmond, Carbon-dioxide and oxygen-isotope anomalies in the mesosphere and stratosphere, *Science*, *270*, 969–972, 1995a.

Thiemens, M. H., T. L. Jackson, and C. A. M. Brenninkmeijer, Observation of a mass-independent oxygen isotopic composition in terrestrial stratospheric CO_2, the link to ozone chemistry, and the possible occurrence in the Martian atmosphere, *Geophys. Res. Lett.*, *22*, 255–257, 1995b.

von Caemmerer, S., and G. D. Farquhar, Some relationships between the biochemistry of photosynthesis and the gas exchange of leaves, *Planta*, *153*, 376–387, 1981.

Weston, R. E., Anomalous or mass-independent isotope effects, *Chem. Rev.*, *99*, 2115–2136, 1999.

White, J. W. C., Stable hydrogen isotope ratios in plants: A review of current theory and some potential applications, in *Stable Isotopes in Ecological Research*, edited by P. W. Rundel, J. R. Ehleringer, and K. A. Nagy, pp. 142–162, Springer-Verlag, New York, 1989.

Yakir, D., J. A. Berry, L. Giles, and C. B. Osmond, Isotopic heterogeneity of water in transpiring leaves: Identification of the component that controls the $\delta^{18}O$ of atmospheric O_2 and CO_2, *Plant Cell Environ.*, *17*, 73–80, 1994.

Yung, Y., W. DeMone, and J. P. Pinto, Isotopic exchange between carbon dioxide and ozone via $O(^1D)$ in the stratosphere, *Geophys. Res. Lett.*, *18*, 13–16, 1991.

Zhang, C., D. A. Dazlich, D. A. Randall, P. J. Sellers, and A. S. Denning, Calculation of the global land surface energy, water, and CO_2 fluxes with an off-line version of SiB2, *J. Geophys. Res.*, *101*, 19,061–19,075, 1996.

Zipf, E. C., and P. W. Erdman, Studies of trace constituents in the upper stratosphere and mesosphere using cryogenic whole sampling techniques, in *NASA's Upper Atmosphere Research Program* (*UARP*) *and Atmospheric Chemistry Modeling and Analysis Program* (*ACMAP*)*, Research Summaries 1992–1993*, U. S. Gov. Print. Off., Washington, D. C., 1994.

B. Barnett, M. L. Bender, and M. B. Hendricks, Department of Geosciences, Princeton University, Guyot Hall, Princeton, NJ 08544, USA. (bbarnett@princeton.edu; bender@princeton.edu; mhendric@princeton.edu)

T. Blunier, Climate and Environmental Physics, Physics Institute, University of Bern, Sidlerstrasse 5, CH-3012 Bern, Switzerland. (blunier@climate.unibe.ch)